molecular pharmaceutics

Article

pubs.acs.org/molecularpharmaceutics

Characteristics of Artemether-Loaded Poly(lactic-*co*-glycolic) Acid Microparticles Fabricated by Coaxial Electrospray: Validation of Enhanced Encapsulation Efficiency and Bioavailability

Farhana Akbar Mangrio,[†,‡,▽] Pankaj Dwivedi,[‡,▽] Shuya Han,[‡] Gang Zhao,[*,†] Dayong Gao,[†,⊥] Ting Si,[*,‡] and Ronald X. Xu[*,‡,§]

[†]Department of Electronic Science and Technology, University of Science and Technology of China, Hefei 230027, China

[‡]School of Engineering Science, University of Science and Technology of China, Hefei 230027, China

[§]Department of Biomedical Engineering, The Ohio State University, Columbus, Ohio 43210, United States

[⊥]Department of Mechanical Engineering, University of Washington, Seattle, Washington 98195, United States

Supporting Information

ABSTRACT: Artemether is one of the most effective drugs for the treatment of chloroquine-resistant and *Plasmodium falciparum* strains of malaria. However, its therapeutic potency is hindered by its poor bioavailability. To overcome this limitation, we have encapsulated artemether in poly(lactic-*co*-glycolic) acid (PLGA) core−shell microparticles (MPs) using the coaxial electrospray method. With optimized process parameters including liquid flow rates and applied electric voltages, experiments are systematically carried out to generate a stable cone-jet mode to produce artemether-loaded PLGA-MPs with an average size of 2 μm, an encapsulation efficiency of 78 ± 5.6%, and a loading efficiency of 11.7%. The in vitro release study demonstrates the sustained release of artemether from the core−shell structure in comparison with that of plain artemether and that of MPs produced by single-axial electrospray without any relevant cytotoxicity. The in vivo studies are performed to evaluate the pharmacokinetic characteristics of the artemether-loaded PLGA-MPs. Our study implies that artemether can be effectively encapsulated in a protective shell of PLGA for controlled release kinetics and enhanced oral bioavailability.

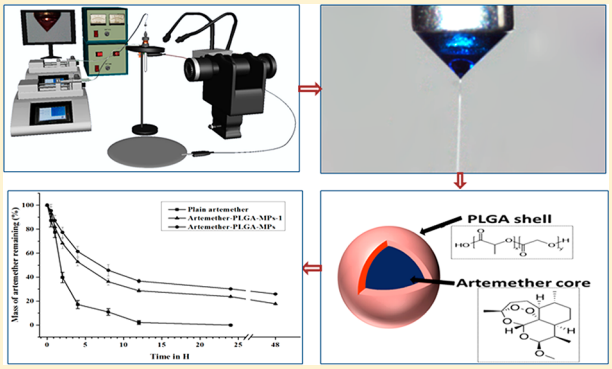

KEYWORDS: *coaxial electrospray, artemether, microencapsulation, bioavailability, drug delivery*

1. INTRODUCTION

Malaria is a life-threatening parasitic infection instigated by *Plasmodium* protozoan parasites. Each year, more than 200 million people in the world are infected by malaria, leading to an estimated 438,000 deaths.[1] Although chloroquine represents the classic treatment of malaria, some strains such as *Plasmodium* (P) *falciparum*, develop chloroquine resistance and are difficult to treat effectively. For patients with chloroquine-resistant malaria, artemisinin and its derivatives represent a promising treatment option.[2] Also called dihydroartemisinin methyl ether, artemether is a form of artemisinin semisynthetic derivative first extracted from *Artemisia annua* L. in 1971.[3] The artemether has blood schizonticidal activity. The putative mechanism of action of artemether states the interface of heme iron and peroxide of artemether, a hemoglobin degradation byproduct, which is produced by the action of the enzyme on hemoglobin proteins into amino acids. The result of this interface causes the formation of reactive oxygen species (ROS) or carbon-centered free radicals, which can possibly be toxic. These oxygen radicals cause inhibition of digestive vacuole cysteine protease of *Plasmodium* strains, a reason for malaria. The hemoglobin accumulates in parasites when treated with artemether, and the formation of hemozoin is also inhibited.[4] It also has antiparasitic activity against *P. vivax*, chloroquine-resistant and -sensitive *P. falciparum* strain, and also finds its application in cerebral malaria management.[5] As per guidelines, artemether is the drug of choice for the treatment of *falciparum* malaria attributable to its potency and rapid action.[6]

At present, artemether is prepared in either an oil formulation (for intramuscular injection) or tablet formulation (for oral delivery). The oil formulation is highly lipophilic, with a partition coefficient value of 3.07, and is relatively stable in biological fluids. However, the current intramuscular drug delivery method is painful and has slow and erratic absorption.[7]

Received: October 1, 2017
Revised: October 24, 2017
Accepted: November 2, 2017
Published: November 2, 2017

DOI: 10.1021/acs.molpharmaceut.7b00862
Mol. Pharmaceutics 2017, 14, 4725−4733

In terms of oral delivery of artemether, the resulting bioavailability is poor (35−40%), and the therapeutic half-life is short (3 h), partially due to its low aqueous solubility and the degradation by stomach acids.[8,9] In comparison with the aforementioned drug delivery routes, intravenous (i.v.) administration of artemether may potentially achieve profound anti-infection activity.[10] Moreover, encapsulating artemether in micro- and nanoparticles of biodegradable materials such as poly(lactic-*co*-glycolic) acid (PLGA) may further facilitate sustained drug release for enhanced bioavailability.[11−14] As a commonly used drug delivery carrier, PLGA has been widely used in many diagnostic and therapeutic applications, such as dentistry, orthopedic surgery, cosmeceuticals, ophthalmologic, oncological, cardiovascular diseases, theranostics, transdermal drug delivery, targeted drug delivery, and also in other medical applications.[15−17] Emulsification is one of the most commonly used processes for producing PLGA micro- or nanoparticles.[16,18] However, this process has multiple limitations that lead to fractional drug release and instability of encapsulated drugs.[19] For example, the removal of organic solvents during the process and the acidic environment may contribute to the instability of the produced particles. Protein unfolding and aggregation is also an associated problem with PLGA carriers in the delivery of biologically active proteins.[20]

In comparison with emulsification, electrospray has a unique advantage for producing monodisperse drug-loaded micro- and nanoparticles with high encapsulation efficiency (% EE) and controllable drug release profiles.[21] The process is based on the formation of a cone jet by electrostatic forces as a liquid meniscus flows out from a capillary tip in an elevated electrical field and ultimately breaks into preliminary droplets.[22] A single-axial electrospray process mixes the therapeutic components in a carrier matrix without a protective shell, leading to a suboptimal drug release profile. In 2002, Loscertales et al. first introduced the coaxial electrospray (CES) process, where MPs with a core−shell structure and a particle size ranging from 0.15 to 10 μm were produced by means of the coaxial jet of two immiscible liquids. The CES process is able to encapsulate a variety of proteins and drugs in a core−shell structure with high EE and minimal loss of biological activity.[23,24] Recently, we improved the CES process to encapsulate curcumin in PLGA-MPs for sustained drug release.[25]

This study reports the CES strategy to produce artemether-loaded PLGA-MPs for enhanced bioavailability in malarial therapy. The operating parameters of the process, such as the applied electric voltage, the inner and outer liquid flow rates, and the coaxial needle configurations, are carefully studied to generate a stable coaxial cone-jet mode for uniform size distribution of the PLGA-MPs. The core−shell structure and the morphology of the PLGA-MPs are evaluated by scanning electron microscopy (SEM) and confocal laser microscopy. Both in vitro and in vivoexperiments are carried out to evaluate the cytotoxicity and artemether release profile of the fabricated PLGA-MPs.

2. MATERIALS AND METHODS

2.1. Materials. Artemether ($C_{16}H_2O_5$) was purchased from Shanxi's Natural Products Co., Ltd. (Shanxi Province, China). PLGA (50:50, MW = 10000−20000) and PLGA (50:50, MW = 50000−70000) were purchased from Shandong Institute of Medical Instrument (Shandong, China). Nile red, coumarin-6, and acetonitrile (99.9% HPLC grade) were procured from Sigma-Aldrich Chemistry (USA). Deionized water was obtained using a pure infinity water purification system (Barnstead International, Dubuque, IA).

2.2. Methods. *2.2.1. Preparation of the Outer and Inner Solutions.* Two different solutions, serving as the outer and inner phases, were prepared. The outer solution of the CES process consisted of 4% w/v PLGA (MW = 10000−20000) in acetonitrile. The inner solution of the CES process consisted of 20.10 mM artemether with 1% w/v PLGA (MW = 50000−70000) in acetonitrile. For the single axial electrospray process, the solution consisted of 4% w/v PLGA (MW = 10000−20000) with 20.10 mM artemether in acetonitrile. As the control, blank PLGA-MPs without encapsulation of artemether were also prepared.

2.2.2. Experimental Setup for the CES Process. The setup of the CES process used for the preparation of PLGA-MPs is illustrated in Figure 1(a). The experimental setup consists of a coaxial needle as a key parameter of the setup, a twin syringe pump (Pump 33, Harvard Apparatus, MA, USA), and two high voltage DC power supplies (positive and negative voltages, Gamma High Voltage Research, Inc., FL, USA). The positive electrode is connected to the coaxial needles, and the negative electrode is connected to the aluminum plate (collector) by a crocodile clip for the collection of the PLGA-MPs. The coaxial cone jet is captured by a CCD camera (Allied Vision Technologies, Inc., MA) and a microscope under illumination of a splash light source. The coaxial needle consists of an inner needle (inner diameter: 0.26 mm; outer diameter: 0.51 mm) and an outer needle (inner diameter: 0.84 mm; outer diameter: 1.27 mm); for higher concentricity, the outer surface of the inner needle is welded by a laser beam in the welding process (pulsed Nd: YAG laser, 1 Hz, 300 W averaged output) with

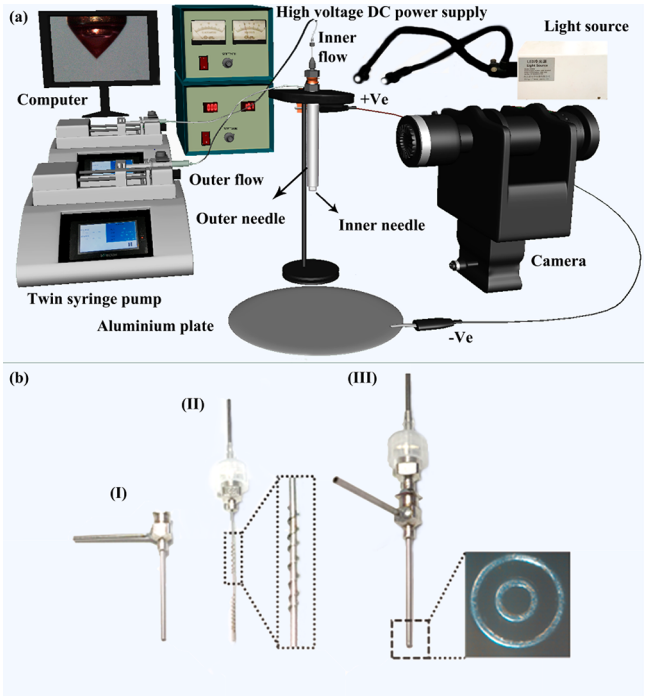

Figure 1. (a) CES setup consists of the coaxial needles, twin syringe pump, high voltage DC power supplies with a positive and negative electrode connected with crocodile clips, aluminum plate microscopic lens combined with CCD camera, computer, and light source. (b) Coaxial needle: (I) outer needle, (II) inner needle, and (III) assembly of the coaxial needle.

DOI: 10.1021/acs.molpharmaceut.7b00862
Mol. Pharmaceutics 2017, 14, 4725−4733

thin silver wires uniformly distributed in circular ring form, as shown in Figure 1(b). The positions of the inner and outer needles can be easily adjusted in the range of −0.2−0.3 mm in a vertical distance h between their tips.

The artemether-loaded and blank PLGA-MPs were prepared. The inner and outer solutions were extruded through the nozzles of inner and outer needles simultaneously by the twin syringe pump. Each of the solutions was maintained at a constant flow rate of 12 μL/min at a ratio of 1:1 by the twin syringe pump. The distance from the tip of the coaxial needle to a collector (ground) was set to 10 cm. The applied positive voltage V_1 was 10 kV, and the applied negative voltage V_2 was 8 kV. The MPs were collected on an aluminum plate connected to the ground electrode. After collection, the artemether-loaded PLGA-MPs were placed in a vacuum chamber for 2 days to ensure complete evaporation of the residual solvents.

For the comparative studies, we have also prepared the artemether-loaded PLGA-MPs using a single axial electrospray process denoted as artemether-loaded PLGA-MPs-1. This method used the artemether and PLGA solutions at the same concentration except that the coaxial needle was replaced by a single axial needle. The particles prepared by the CES method have been denoted as artemether-loaded PLGA-MPs.

3. MORPHOLOGICAL CHARACTERIZATION

3.1. Scanning Electron Microscopy. Morphologic characteristics of the produced artemether-loaded PLGA-MPs were examined by the GeminiSEM 500 Scanning electron microscope (SEM) system (Carl Zeiss Microscopy Gmbh 73447 Oberkochen, Germany). The particles were mounted on an aluminum stub and processed by the coating of gold−palladium (Au/Pd) for 30 s before SEM imaging.

3.2. Confocal Laser Scanning Microscopy. The core−shell structure of the artemether-loaded PLGA-MPs was verified by Nikon eclipse Ti confocal laser scanning microscopy (CLSM) using Apo TIRF 60 × /1.49 oil. The Nile red (0.01 w %) was used as a fluorescent dye in the outer solution of PLGA, and coumarin-6 (0.01 w %) was used as a fluorescent dye for the inner solution.

3.3. Measurement of the Size Distribution. The size distribution of MPs was determined using dynamic light scattering (DLS) analyzed by Zetasizer (Nano series, Nano-ZS90) measuring the hydrodynamic diameter of small particles in suspension formed at different voltages.

3.4. Differential Scanning Calorimetry (DSC) and Residual Solvent Analysis. DSC was performed using DSCQ2000 V24.10 Build122 (TA Instruments), where artemether, a physical mixture of artemether and PLGA, and artemether-loaded PLGA-MPs were examined. The empty pan was used as a reference, whereas another empty pan served as the sampling pan in which 5 mg samples were placed. A heating speed of 10 °C/min was used, and the sample was kept in a dry nitrogen atmosphere. Samples were examined over the temperature range of 0−150 °C.

Gas chromatography-mass spectroscopy (GC-MS) was performed to evaluate the existence of any residual acetonitrile solvent in PLGA-MPs. The detailed method and description are provided in the Supporting Information.

3.5. Loading Rate (LR) and Encapsulation Efficiency (EE). To determine the LR and EE of artemether in artemether-loaded PLGA-MPs-1 and artemether-loaded PLGA-MPs, we dissolved the known amount of MPs in acetonitrile. The solution obtained was filtered using 0.4 μm size filters. The filtrate was appropriately diluted, and an amount of artemether was estimated using the LC-MS method with standard protocols. Equations below were used to derive loading rate (LR) (%) and encapsulation efficiency (EE) (%).

$$\text{EE (\%)} = \frac{\text{weight of artemether in artemether-loaded PLGA-MPs}}{\text{weight of artemether initially taken}} \times 100$$

$$\text{LR (\%)} = \frac{\text{weight of artemether in artemether-loaded PLGA-MPs}}{\text{weight of artemether-loaded PLGA-MPs}} \times 100$$

3.6. In Vitro Drug Release. In vitro artemether release study was carried out in gastric fluid (pH 1.2) for an initial 2 h followed by intestinal fluid (pH 7.4) for 48 h. The samples having an equivalent amount of artemether in artemether-loaded PLGA-MPs-1, artemether-loaded PLGA-MPs, and plain artemether was dispersed in 5 mL of phosphate-buffered saline (PBS) in a dialysis bag and sealed. The dialysis bags were first immersed in 200 mL of dissolution medium containing gastric fluid (pH 1.2) for 2 h and then into the intestinal fluid (pH 7.4) for 48 h in a beaker. The beaker was kept in a shaker, and the temperature was maintained at 37 °C and shaken at 50 rpm. A sample (2 mL) was withdrawn at predetermined intervals of 0, 0.5, 1, and 2 h. After 2 h, the dialysis bag was removed from the gastric fluid and placed in 200 mL of PBS. The samples were withdrawn for the next 4, 6, 9, 12, 24, and 48 h. For the sink condition to be maintained, release medium was exchanged with an equal volume of fresh release medium. The concentration of released artemether was determined by LC-MS/MS as mentioned previously.

3.7. Liquid Chromatography Mass Spectroscopy. The Thermo Scientific LC-MS/MS System (San Jose, USA) was used for analyzing the samples of artemether, which consisted of an Acela MS Pump-Plus and Acela autosampler. High-resolution LTQ-Orbitrap XL operated in positive ion mode was performed for detection. Analyte separation was achieved using a C18 RP column (150 mm × 4.6 mm, 5 μm; Bellefonte, USA). The chromatographic data was acquired on Thermo Tune Plus software. Filtered with 0.22 m Millipore filter (Billerica, USA) and degassed ultrasonically for 15 min, the mobile phase along with acetonitrile and water with 0.1% formic acid at a ratio of 80:20 (v/v) was allowed to run in isocratic mode at 300 μL/min flow rate. The analytical column was kept at 35 °C. The MS was operated in SIM mode with a capillary temperature set at 375 °C, and the source and capillary voltages were 4.5 and 35 kV, respectively. The auxiliary and sheath gases were 15 and 50 arbitrary units, respectively. For accurate determination, the m/z ranges set for artemether were 267.14−267.16 and 221.16−221.18 amu.

3.8. Cell Culture and Maintenance. The intestinal Caco2 cell line was used. The cells were grown in HyClone's modified RPMI medium appended with 20% fetal bovine serum (FBS) and 1% penicillin-streptomycin solution (Hyclone Laboratories) kept in an incubator at 37 °C with 5% CO_2 and 90% humidity.

3.9. Cytotoxicity. Cytotoxicity studies were carried out using 3-(4,5-dimethylthiazol-2-yl)-2,5-diphenyltetrazolium bromide (MTT) assay on the intestinal Caco2 cell line for the safety analysis of excipients used in the preparation of artemether-loaded PLGA-MPs. Caco-2 cell suspensions were seeded in 96-well plates at 1 × 10^6 cells/well in RPMI medium and allowed to adhere at 37 °C for 24 h. After that, the culture medium was replaced with fresh medium, and the cells were treated with 10 mg of blank PLGA-MPs; no test solution was

DOI: 10.1021/acs.molpharmaceut.7b00862
Mol. Pharmaceutics 2017, 14, 4725−4733

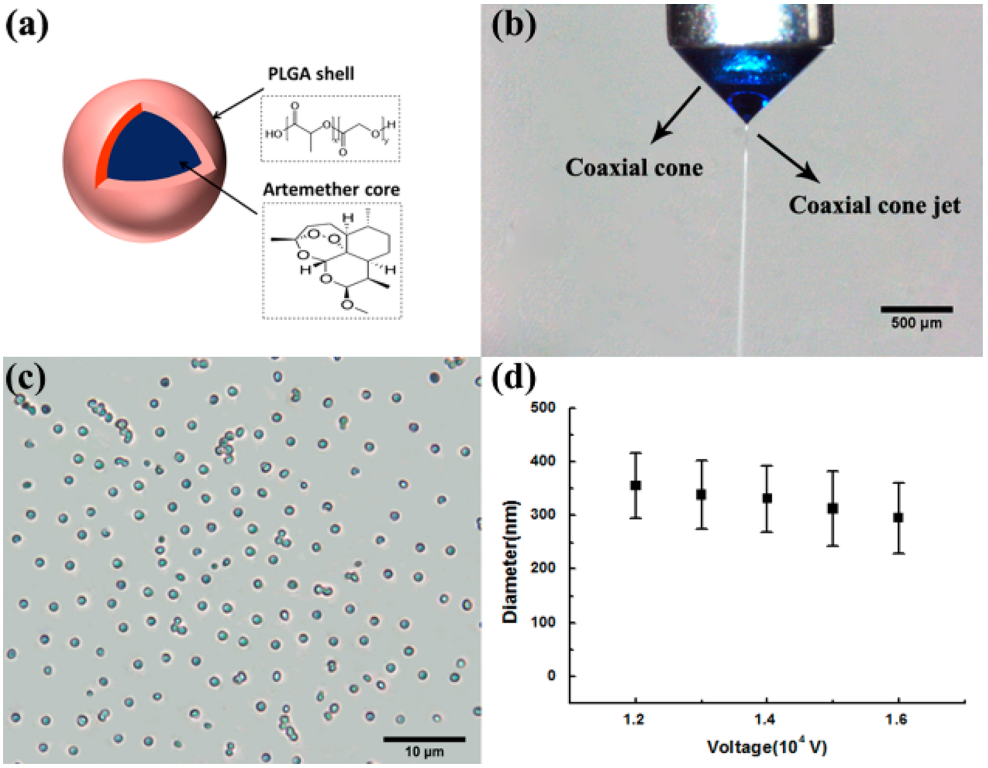

Figure 2. (a) Artemether-loaded PLGA-MPs and (b) stable coaxial cone and jet. Outer and inner flow rate at a 1:1 ratio of 12 μL/min; coaxial tip to collector plate distance (h) of 10 cm; positive voltage V_1 = 10 kV, negative voltage V_2 = 8 kV. (c) Microscopic image of collected artemether-loaded PLGA-MPs on a glass slide. (d) Influence of applied positive voltage V_1 on mean diameter of the MPs collected in water after applying diverse positive voltage of V_1 = 12−16 kV and V_2 = −8 kV.

added for control. The cells were incubated for 24 and 48 h, after which the cell viability was assessed by adding 100 μL of 5 mg/mL of MTT solution and incubating again at 37 °C for 4 h. For solubilization of the formazan crystals, 100 μL of dimethyl sulfoxide (DMSO) was used, and the cell plate was placed on a shaker for 30 min for agitation. The multiwell scanning spectrophotometer (MRX Microplate Reader, Dynatech Laboratories Inc., Chantilly, VA, USA) was used to measure the optical density at a wavelength of 570 nm.

3.10. In Vivo Pharmacokinetic Study of Artemether-Loaded PLGA-MPs by LC-MS. Young, adult Wistar rats of either sex were purchased from Beijing Vital River Laboratory Animal Technology Co., Ltd. (Beijing, China). The adult Wistar rats were kept in the Animal Care Centre Facility of the University of Science and Technology of China (USTC). Rats were housed in well-ventilated cages at room temperature (24 ± 2 °C) and 40−60% relative humidity. Approval from the Local Animal Ethics Committee of USTC (under Protocol No. USTCACUC1501014) was sought and approved, and the study protocols were followed before commencement of the studies.

Wistar rats with weights of 250 ± 20 g were divided into three groups having six animals in each group. Group I was administered with artemether aqueous suspension in 1% Tween 80. Group II was administered with artemether-loaded PLGA-MPs-1. Group III was loaded with artemether-loaded PLGA-MPs. All of the rats were administered with an equivalent dose of artemether (i.e., 10 mg of artemether per kg body weight of rats). This 10 mg/kg dose of artemether corresponds to the artemether present in the formulation either in PLGA-MPs or in artemether suspension. The plasma concentration of the drug was monitored using the above-mentioned LC-MS. After the single administration to each animal of different groups, blood was collected from the retro-orbital plexus of rats into microfuge tubes containing heparin at predetermined intervals of 15, 30, 60, 120, 240, 480, 720, and 1440 min of postdosing. Plasma was isolated from blood after centrifugation at 5,000 rpm for 10 min and stored at −80 ± 10 °C (frozen) until analysis. Plasma samples were analyzed after 100 μL of plasma sample was extracted using a liquid−liquid extraction method. A mixture of 1 mL of 1:1 hexane:ethyl acetate (v/v) was added to 100 μL of plasma and vortexed for 5 min followed by centrifugation at 2000 rpm for 5 min on a Zonkia HC-3018 high-speed centrifuge (China). The organic layer was separated, and the procedure was repeated three times. At the end, the organic layer of all three extractions was combined and evaporated to dryness under vacuum in speed vac concentrator (Savant Instrument, Farmingdale, USA). The residue was reconstituted with 100 μL of acetonitrile and was used for analysis.

The data obtained were analyzed using the noncompartmental model of WinNonlin (version 5.1, Pharsight Corporation, Mountain View, USA). Visual inspection of the experimental data was used to obtain the maximum plasma concentration (C_{max}) and the time to reach the maximum plasma concentration (T_{max}). The area under the curve (AUC) was also calculated using the trapezoidal rule.

3.11. Statistical Analysis. The results obtained from the experiments were analyzed for their significance using one-way analysis of variance (ANOVA) followed by the Turkey−Kramer multiple comparison tests using Graph Pad Instat software (Graph Pad Software Inc., CA, USA). $p < 0.05$ denotes

DOI: 10.1021/acs.molpharmaceut.7b00862
Mol. Pharmaceutics 2017, 14, 4725−4733

Table I. Physicochemical Characterization of Some Artemether-Loaded PLGA-MPs-1 and Artemether-Loaded PLGA-MPs Formulations[a]

formulation	% encapsulation efficiency	% loading efficiency	average particle size (μm)	polydispersity index	zeta potential (mV)
artemether-loaded PLGA-MPs-1	69 ± 3.7	10.35	1.18 ± 0.17	0.241 ± 0.07	−17.54 ± 0.19
artemether-loaded PLGA-MPs	78 ± 5.6	11.7	2.56 ± 0.24	0.199 ± 0.08	−20.44 ± 0.26

[a]Values are expressed as mean ± SD (n = 3).

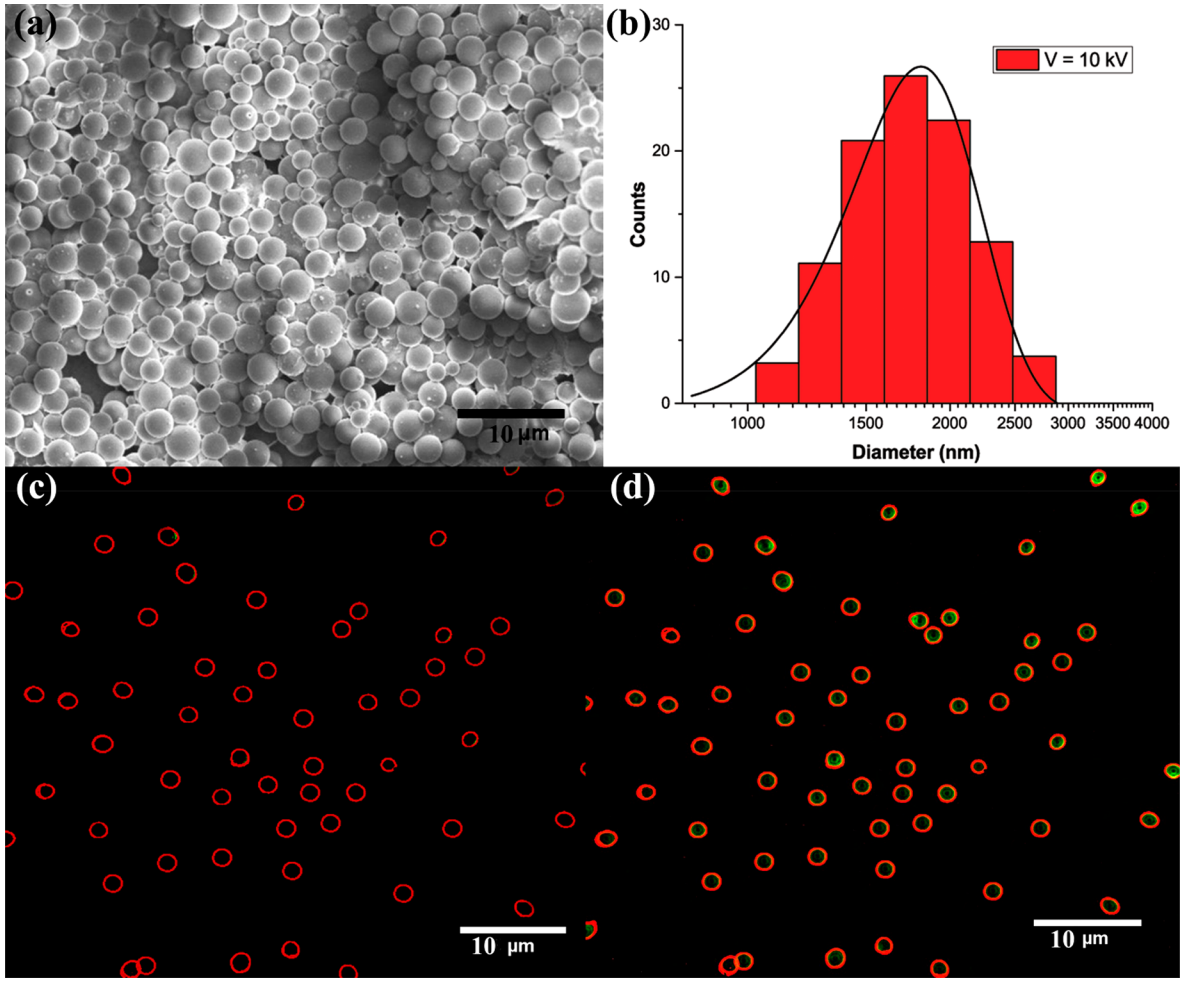

Figure 3. (a) SEM image depicting the smooth morphology and monodispersity of artemether-loaded PLGA-MPs obtained from CES. (b) Size distribution of the MPs for the applied positive voltages of V_1 = 10 kV and V_2 = −8 kV. The outer and inner flow rates were 12 μL/min with a 1:1 ratio. (c) Intraparticle artemether (drug) distribution depicted by confocal laser microscopic image using 60×/1.49 oil emulsion lens showing the core−shell entrapment of the outer Nile red (0.01 wt %) fluorescent dye in PLGA solution and inner core of coumarin-6 green (0.01 wt %) fluorescent dye in artemether solution. Microscopic images depicting the shell shape. (d) Drug (artemether) entrapment in the core phase (green coumarin-6) of the MPs.

significance in all cases. The results are expressed as mean ± SD (n = 3).

RESULTS AND DISCUSSION

4.1. Fabrication of Artemether-Loaded PLGA-MPs.

The experimental setup is depicted in Figure 1 (a), which shows the fabrication of artemether-loaded PLGA-MPs through a stable coaxial cone-jet mode of the CES process. When the PLGA and artemether solutions flow through the coaxial needle, they end up in the formation of small droplets under the influence of an applied voltage. These tiny droplets dry during the time-of-flight before they reach the collector. The process parameters used in the preparation of MPs, such as the distance between the two electrodes, applied voltage, liquid flow rates, and concentrations of the PLGA and artemether solution have been critically optimized for the formation of the stable cone. These parameters have been thoroughly optimized, which resulted in the uniform, stable, and high artemether-encapsulated PLGA-MPs following our previous experimental processes.[25]

In the inner solution, 1% w/v PLGA (MW = 50000−70000) was added with artemether in acetonitrile to increase the viscosity and encapsulation efficiency. The acetonitrile was chosen for the inner and outer solvents based on the solubility of the polymer and the drug. We have encapsulated artemether in PLGA-MPs by the CES process. With the current experimental setup, we were able to achieve the production rate of 40 mg per hour for artemether-loaded PLGA-MPs. By

DOI: 10.1021/acs.molpharmaceut.7b00862
Mol. Pharmaceutics 2017, 14, 4725−4733

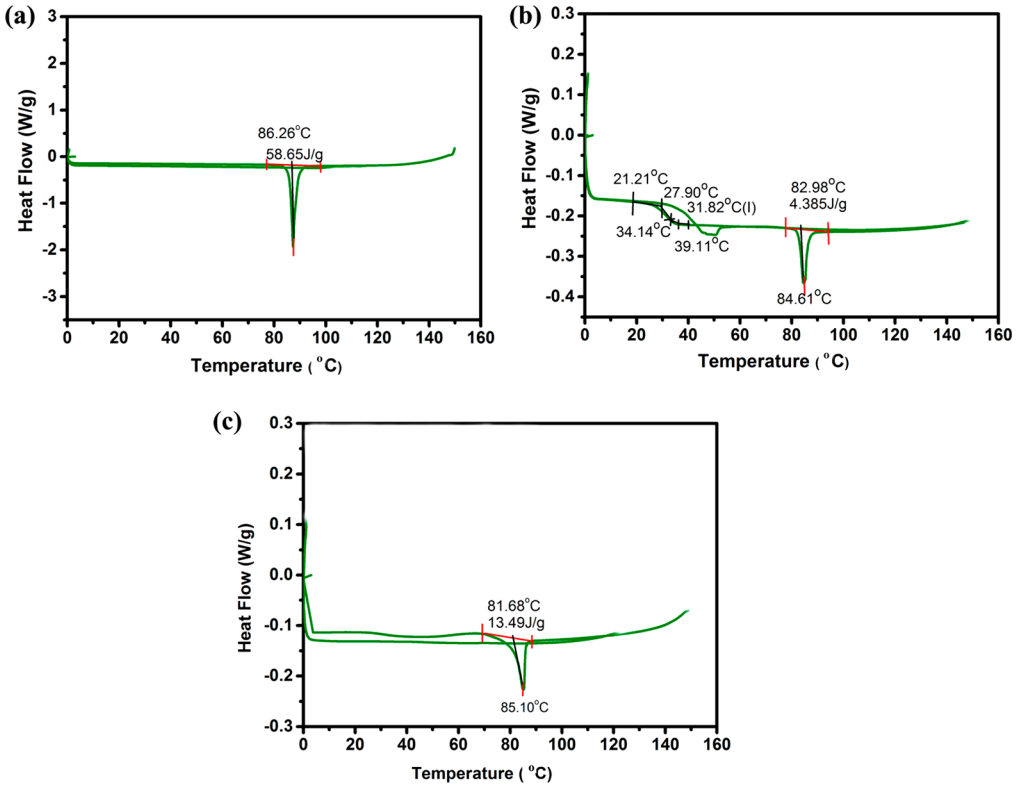

Figure 4. DSC curves of (a) artemether, (b) a physical mixture of artemether and PLGA, and (c) artemether-loaded PLGA-MPs.

designing an array of coaxial CES needles, it is possible to scale up the microencapsulation process for mass production of artemether-loaded PLGA-MPs.

4.2. Characterization of Artemether-Loaded PLGA-MPs. Figure 2(a) illustrates the core−shell structure of the artemether-loaded PLGA-MPs. This core−shell structure is produced by a CES process where the inner and outer liquids flow through the coaxial needle and form the stable cone-jet mode, as shown in Figure 2(b). The cone-jet further breaks into uniform droplets, as shown by the microscopic image in Figure 2(c). The change in applied positive electric voltage played a critical role in the mean diameter of the droplet size. The droplets were collected after applying diverse positive voltage from 12 to 16 kV. The hydrodynamic diameter of small particles formed by the effect of different voltages was analyzed using Zetasizer (Nano series, Nano-ZS90). The increase in the voltage caused a reduction in the diameter of the prepared MPs, as shown in Figure 2(d). The data are represented in Table I. The mean diameter of artemether-loaded PLGA-MPs was 2.56 ± 0.21 μm, which was obtained at an applied positive voltage of 10 kV and applied negative voltage of −8 kV. The size and surface morphology were confirmed as spherical and smooth by the SEM images and the Zetasizer measurement in Figure 3(a, b). The zeta potential of the particles was found to be −20.44 ± 0.26 mV.

4.3. Formation of Core−Shell-Structured PLGA-MPs. The core−shell structure of the artemether-loaded PLGA-MPs was confirmed by CLSM, where the outer liquid of the PLGA solution was stained with Nile red and the inner liquid of artemether solution was stained with coumarin-6 green for confocal fluorescence imaging of the core−shell structure, as illustrated in Figure 3(c,d).

4.4. DSC Experiment and Residual Solvent Analysis by GC-MS. The investigation of drug−polymer interactions was carried out using a DSC instrument that could detect the change in physical properties when subjected to an elevated temperature at a constant rate with reference to the standard. Panels a−c in Figure 4 show the DSC curves for pure artemether, a physical mixture of PLGA and artemether, and artemether-loaded PLGA-MPs, respectively. The DSC curves of the three samples show an endothermic peak corresponding to a melting point of 87.36 °C, indicating the crystalline nature of artemether. The result suggests that artemether regains its crystalline nature and maintains its stability even after encapsulation in the PLGA-MPs.

The GC-MS results show no residual acetonitrile in the artemether-loaded PLGA-MPs (Figure S1). Acetonitrile is a class 2 solvent in pharmaceutical products with a permissible limit of 410 ppm. This confirms that our artemether-loaded PLGA-MPs follow the recommendations of the International Council for Harmonization of Technical Requirements for Pharmaceuticals for Human Use (ICH) guideline of residual solvent and thus are completely safe and free of any residual solvent.

4.5. Encapsulation Efficiency and Cytotoxicity. The %EE of artemether-loaded PLGA-MPs fabricated by coaxial electrospray was found to be 78 ± 5.6%, whereas the %EE of artemether-loaded PLGA-MPs-1 was <70% fabricated by single axial electrospray. The %LE of artemether-loaded PLGA-MPs fabricated by coaxial electrospray was found to be 11.7%, whereas the %LE of artemether-loaded PLGA-MPs-1 was found to be 10.35%.

Cytotoxicity of the blank PLGA-MPs without drug was evaluated in Caco2 cells. We have chosen Caco-2 cells because our formulation has been designed for oral administration and

DOI: 10.1021/acs.molpharmaceut.7b00862
Mol. Pharmaceutics 2017, 14, 4725−4733

Caco-2 cells represent the best model for endothelial cells of a normal intestine. Although PLGA has been approved by the US FDA as nontoxic, this study was conducted to evaluate any potential toxicity of our final formulation. Any toxicity caused by residual organic solvent acetonitrile in PLGA-MPs was evaluated. The results demonstrated that the difference between the control group (untreated cells) and the cells treated with blank PLGA-MPs was not significant (<10%), revealing the safety of our formulation

4.6. In Vitro Release Profile of Artemether in Artemether-Loaded PLGA-MPs. Figure 5 compares the

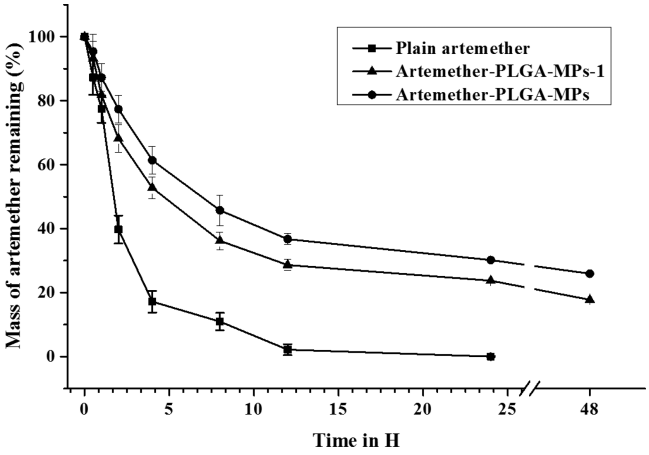

Figure 5. In vitro release of artemether from artemether-loaded PLGA-MPs-1, artemether-loaded PLGA-MPs, and plain artemether.

release profiles of artemether released from artemether-loaded PLGA-MPs, artemether-loaded PLGA-MPs-1, and plain artemether. As observed from the figure, the amount of artemether released initially from both MPs was more than 20% of the drug within 2 h. This could be attributed to the amount of artemether that diffused out toward the shell of the particles during the time of evaporation of the solvent, and this outer shell artemether was released during the initial time points. Later it was observed that artemether-loaded PLGA-MPs-1 had a higher release rate in comparison with that of artemether-loaded PLGA-MPs for which sustained release was observed. This might be due to the protected shell presented on the surface of artemether-loaded PLGA-MPs, which significantly reduced the release rate of artemether. The plain drug was released more than 60% in the initial 4 h, whereas complete release of plain drug was observed within 12 h. The artemether-loaded PLGA-MPs showed comparatively more sustained release than that of artemether-loaded PLGA-MPs-1, which might be caused by the complete encapsulation of artemether in the core with a hard shell of PLGA.

The results suggest that the acid present in the stomach, which causes degradation of initially exposed artemether, could be reduced by core−shell encapsulation. The acid might break the endoperoxide bridge (responsible for artemether antimalarial activity) of artemether and may result in reduced antimalarial activity. The artemether has been well-encapsulated in the core of the PLGA-MPs and has a protected shell, which influences the dissolution profile of artemether allowing it to release in a sustained manner. This sustained release of the artemether will protect it from initial exposure to stomach acid.

4.7. Pharmacokinetic Study of Artemether-Loaded PLGA-MPs in Adult Wistar Rats. Figure 6 shows the plasma

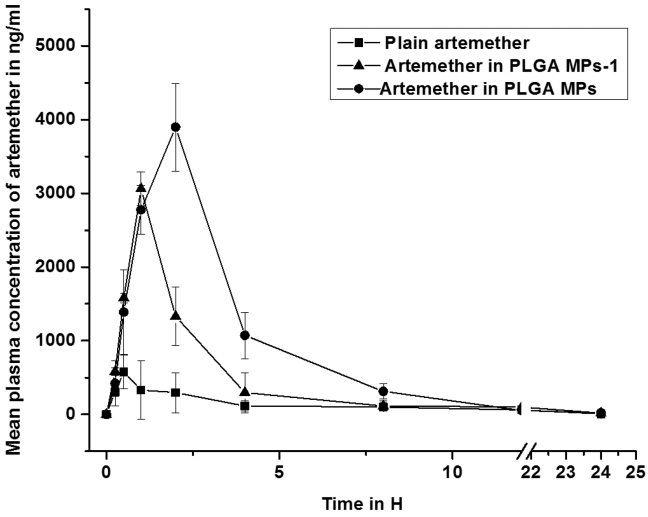

Figure 6. Mean plasma concentration−time profile of artemether upon oral administration. Data are represented as mean ± SD (n = 3).

concentration−time profiles in adult Wistar rats after oral administration of artemether in aqueous suspension, artemether-loaded PLGA-MPs-1, and artemether-loaded PLGA-MPs, respectively. According to the pharmacokinetic data presented in Table II, the bioavailability of artemether-loaded PLGA-MPs (prepared by CES) was significantly higher than that of artemether-loaded PLGA-MPs-1 (prepared by single electrospray) and as well as plain artemether. C_{max} and AUC_{0-t} for all the artemether-loaded PLGA-MPs were significantly higher than those for artemether in aqueous suspension and artemether-loaded PLGA-MPs-1. The AUC in the case of artemether-loaded PLGA-MPs (AUC_{0-t} = 13869.45 ± 587.05 h ng mL^{-1}) was significantly higher (p < 0.05) than that of artemether-loaded PLGA-MPs-1 (AUC_{0-t} = 7507.31 ± 319.42 h ng mL^{-1}) and artemether aqueous suspension (AUC_{0-t} = 2323.12 ± 287.25 h ng mL^{-1}); $t_{1/2}$ of artemether-loaded PLGA-MPs was found to be 3.38 ± 1.69 h, whereas artemether-loaded PLGA-MPs-1 had $t_{1/2}$ = 3.56 ± 1.47 h and artemether aqueous suspension had $t_{1/2}$ = 4.08 ± 1.58 h. The C_{max} of artemether-loaded PLGA-MPs (3896.66 ± 384.53 ng/mL) was also significantly higher (p < 0.05) than that of artemether-loaded PLGA-MPs-1 (3061.49 ± 327.21 ng/mL) and artemether in aqueous suspension (576.50 ± 57.72 ng/mL), whereas T_{max} of artemether-loaded PLGA-MPs-1 and artemether-loaded PLGA-MPs were 1 and 2 h, respectively.

The results revealed that directly delivered artemether was rapidly absorbed and reached its maximum concentration within 0.5 h. In comparison, artemether-loaded PLGA-MPs-1 and artemether-loaded PLGA-MPs achieved the maximum concentrations in 1 and 2 h, respectively. The results indicated the sustained release of artemether from artemether-loaded PLGA-MPs extended its therapeutic half-life and increased its bioavailability.

CONCLUSIONS

Artemether-loaded PLGA-MPs of around 2 μm in diameter were successfully prepared using a coaxial electrospray (CES) process. The particles have clearly defined core−shell structure and a high encapsulation efficiency of 78.56%. The cell viability assay revealed that the carrier PLGA material induced minimal cytotoxicity. The in vivo experiment demonstrated that encapsulating artemether in PLGA microcapsules effectively

DOI: 10.1021/acs.molpharmaceut.7b00862
Mol. Pharmaceutics 2017, 14, 4725−4733

Table II. Pharmacokinetic Parameters of Artemether-Loaded PLGA-MPs-1 and Artemether-Loaded PLGA-MPs Present in Artemether in Aqueous Suspension, Upon Oral Administration[a]

parameter	artemether aqueous suspension	artemether-loaded PLGA-MPs-1	artemether-loaded PLGA-MPs
$t_{1/2}$ (h)	4.08 ± 1.58	3.56 ± 1.47	3.38 ± 1.69[b]
AUC_{0-t} (h ng mL^{-1})	2323.12 ± 287.25	7507.31 ± 319.42	13869.45 ± 587.05[b,c]
C_{max} (ng/mL)	576.50 ± 57.72	3061.49 ± 327.21	3896.66 ± 384.53[b]
T_{max} (h)	0.5	1	2

[a]Data represented as mean ± S.D (n = 4). [b]Significantly different compared to artemether in aqueous suspension ($p < 0.05$). [c]Significantly different compared to artemether in artemether-loaded PLGA-MPs-1 ($p < 0.05$).

enhanced the bioavailability of artemether. Through these experiments, we conclude that CES is a reliable method for preparing a delivery system that can enhance the bioavailability of artemether in malaria treatment. This formulation can be given with lumefantrine to achieve better efficacy in malaria treatment. In the future, it is also feasible to fabricate artemether/lumefantrine core−shell MPs by the CES method with improved therapeutic potency. Further animal and clinical investigations are necessary before the process can be implemented in a clinical setting.

■ ASSOCIATED CONTENT

Supporting Information

The Supporting Information is available free of charge on the ACS Publications website at DOI: 10.1021/acs.molpharmaceut.7b00862.

Experimental details and spectroscopic and crystallographic data for $KInSn_2S_6$ (PDF)

■ AUTHOR INFORMATION

Corresponding Authors

*E-mail: zhaog@ustc.edu.cn.
*E-mail: tsi@ustc.edu.cn.
*E-mail: xu.202@osu.edu.

ORCID

Gang Zhao: 0000-0002-0201-1825
Ronald X. Xu: 0000-0003-2486-5677

Author Contributions

▽F.A.M. and P.D. contributed equally to this work.

Notes

The authors declare no competing financial interest.

■ ACKNOWLEDGMENTS

The authors are thankful to the School of Life Science at the University of Science and Technology of China for providing various facilities for conducting animal experiments. This research work was supported by National Natural Science Foundation of China (Nos.11472270, 81327803, 51476160, 51528601, 11621202, and 11722222) and the Fundamental Research Funds for the Central Universities.

■ REFERENCES

(1) The World Health Organization, *World malaria report, 2015*; World Health Organization, 2016.
(2) Wongsrichanalai, C.; Pickard, A. L.; Wernsdorfer, W. H.; Meshnick, S. R. Epidemiology of drug-resistant malaria. *Lancet Infect. Dis.* **2002**, *2* (4), 209−218.
(3) Webster, H. K.; Lehnert, E. K. Chemistry of artemisinin: an overview. *Trans. R. Soc. Trop. Med. Hyg.* **1994**, *88*, 27−29.
(4) Cui, L.; Su, X.-z. Discovery, mechanisms of action and combination therapy of artemisinin. *Expert Rev. Anti-Infect. Ther.* **2009**, *7* (8), 999−1013.
(5) Joshi, M.; Pathak, S.; Sharma, S.; Patravale, V. Design and in vivo pharmacodynamic evaluation of nanostructured lipid carriers for parenteral delivery of artemether: Nanoject. *Int. J. Pharm.* **2008**, *364* (1), 119−126.
(6) The World Health Organization, *Guidelines for the treatment of malaria*; World Health Organization, 2006.
(7) Hien, T. T.; Davis, T. M. E.; Chuong, L. V.; Ilett, K. F.; Sinh, D. X. T.; Phu, N. H.; Agus, C.; Chiswell, G. M.; White, N. J.; Farrar, J. Comparative Pharmacokinetics of Intramuscular Artesunate and Artemether in Patients with Severe Falciparum Malaria. *Antimicrob. Agents Chemother.* **2004**, *48* (11), 4234−4239.
(8) Karbwang, J.; Na-Bangchang, K.; Congpuong, K.; Molunto, P.; Thanavibul, A. Pharmacokinetics, and bioavailability of oral and intramuscular artemether. *Eur. J. Clin. Pharmacol.* **1997**, *52* (4), 307−10.
(9) White, N. J. Assessment of the pharmacodynamic properties of antimalarial drugs in vivo. *Antimicrob. Agents Chemother.* **1997**, *41* (7), 1413−22.
(10) Li, Q.-G.; Peggins, J. O.; Fleckenstein, L. L.; Masonic, K.; Heiffer, M. H.; Brewer, T. G. The Pharmacokinetics and Bioavailability of Dihydroartemisinin, Arteether, Artemether, Artesunic Acid and Artelinic Acid in Rats. *J. Pharm. Pharmacol.* **1998**, *50* (2), 173−182.
(11) Aditya, N. P.; Patankar, S.; Madhusudhan, B.; Murthy, R. S. R.; Souto, E. B. Arthemeter-loaded lipid nanoparticles produced by modified thin-film hydration: Pharmacokinetics, toxicological and in vivo anti-malarial activity. *Eur. J. Pharm. Sci.* **2010**, *40* (5), 448−455.
(12) Agubata, C. O.; Nzekwe, I. T.; Attama, A. A.; Mueller-Goymann, C. C.; Onunkwo, G. C. Formulation, characterization and anti-malarial activity of homolipid-based artemether microparticles. *Int. J. Pharm.* **2015**, *478* (1), 202−22.
(13) Laxmi, M.; Bhardwaj, A.; Mehta, S.; Mehta, A. Development, and characterization of nanoemulsion as carrier for the enhancement of bioavailability of artemether. *Artif. Cells, Nanomed., Biotechnol.* **2015**, *43* (5), 334−44.
(14) Sadat Tabatabaei Mirakabad, F.; Nejati-Koshki, K.; Akbarzadeh, A.; Yamchi, M. R.; Milani, M.; Zarghami, N.; Zeighamian, V.; Rahimzadeh, A.; Alimohammadi, S.; Hanifehpour, Y.; Joo, S. W. PLGA-based nanoparticles as cancer drug delivery systems. *Asian Pacific journal of cancer prevention: APJCP* **2014**, *15* (2), 517−35.
(15) Chan, J. M.; Zhang, L.; Yuet, K. P.; Liao, G.; Rhee, J.-W.; Langer, R.; Farokhzad, O. C. PLGA−lecithin−PEG core−shell nanoparticles for controlled drug delivery. *Biomaterials* **2009**, *30* (8), 1627−1634.
(16) Cohen-Sela, E.; Chorny, M.; Koroukhov, N.; Danenberg, H. D.; Golomb, G. A new double emulsion solvent diffusion technique for encapsulating hydrophilic molecules in PLGA nanoparticles. *J. Controlled Release* **2009**, *133* (2), 90−95.
(17) Kapoor, D. N.; Bhatia, A.; Kaur, R.; Sharma, R.; Kaur, G.; Dhawan, S. PLGA: a unique polymer for drug delivery. *Ther. Delivery* **2015**, *6* (1), 41−58.
(18) Ajalloueian, F.; Tavanai, H.; Hilborn, J.; Donzel-Gargand, O.; Leifer, K.; Wickham, A.; Arpanaei, A. Emulsion Electrospinning as an Approach to Fabricate PLGA/Chitosan Nanofibers for Biomedical Applications. *BioMed Res. Int.* **2014**, *2014*, 475280.

DOI: 10.1021/acs.molpharmaceut.7b00862
Mol. Pharmaceutics 2017, 14, 4725−4733

(19) Houchin, M. L.; Topp, E. M. Chemical degradation of peptides and proteins in PLGA: a review of reactions and mechanisms. *J. Pharm. Sci.* **2008**, *97* (7), 2395−404.
(20) Astete, C. E.; Sabliov, C. M. Synthesis and characterization of PLGA nanoparticles. *J. Biomater. Sci., Polym. Ed.* **2006**, *17* (3), 247−289.
(21) Xie, J.; Wang, C. H. Encapsulation of proteins in biodegradable polymeric microparticles using electrospray in the Taylor cone-jet mode. *Biotechnol. Bioeng.* **2007**, *97* (5), 1278−90.
(22) Karimi Zarchi, A. A.; Abbasi, S.; Faramarzi, M. A.; Gilani, K.; Ghazi-Khansari, M.; Amani, A. Development and optimization of N-Acetylcysteine-loaded poly (lactic-co-glycolic acid) nanoparticles by electrospray. *Int. J. Biol. Macromol.* **2015**, *72*, 764−70.
(23) Loscertales, I. G.; Barrero, A.; Guerrero, I.; Cortijo, R.; Marquez, M.; Ganan-Calvo, A. M. Micro/nano encapsulation via electrified coaxial liquid jets. *Science* **2002**, *295* (5560), 1695−8.
(24) Zhang, L.; Huang, J.; Si, T.; Xu, R. X. Coaxial electrospray of microparticles and nanoparticles for biomedical applications. *Expert Rev. Med. Devices* **2012**, *9* (6), 595−612.
(25) Yuan, S.; Lei, F.; Liu, Z.; Tong, Q.; Si, T.; Xu, R. X. Coaxial Electrospray of Curcumin-Loaded Microparticles for Sustained Drug Release. *PLoS One* **2015**, *10* (7), e0132609.

DOI: 10.1021/acs.molpharmaceut.7b00862
Mol. Pharmaceutics 2017, 14, 4725−4733